Guanylyl cyclase is an ATP sensor coupling nitric oxide signaling to cell metabolism

I. Ruiz-Stewart*, S. R. Tiyyagura*, J. E. Lin*, S. Kazerounian*, G. M. Pitari*, S. Schulz*, E. Martin†, F. Murad†, and S. A. Waldman*‡

*Division of Clinical Pharmacology, Departments of Medicine and Biochemistry and Molecular Pharmacology, Thomas Jefferson University, Philadelphia, PA 19107; and †Department of Integrative Biology and Pharmacology, Institute of Molecular Medicine, University of Texas Health Science Center, Houston, TX 77030

Edited by Louis J. Ignarro, University of California School of Medicine, Los Angeles, CA, and approved November 13, 2003 (received for review August 8, 2003)

Defending cellular integrity against disturbances in intracellular concentrations of ATP ($[ATP]_i$) is predicated on coordinating the selection of substrates and their flux through metabolic pathways (metabolic signaling), ATP transfer from sites of production to utilization (energetic signaling), and the regulation of processes consuming energy (cell signaling). Whereas NO and its receptor, soluble guanylyl cyclase (sGC), are emerging as key mediators coordinating ATP supply and demand, mechanisms coupling this pathway with metabolic and energetic signaling remain undefined. Here, we demonstrate that sGC is a nucleotide sensor whose responsiveness to NO is regulated by $[ATP]_i$. Indeed, ATP inhibits purified sGC with a K_i predicting >60% inhibition of NO signaling in cells maintaining physiological $[nucleotide]_i$. ATP inhibits sGC by interacting with a regulatory site that prefers ATP > GTP. Moreover, alterations in $[ATP]_i$, by permeabilization and nucleotide clamping or inhibition of mitochondrial ATP synthase, regulate NO signaling by sGC. Thus, $[ATP]_i$ serves as a ''gain control'' for NO signaling by sGC. At homeostatic $[ATP]_i$, NO activation of sGC is repressed, whereas insults that reduce $[ATP]_i$, derepress sGC and amplify responses to NO. Hence, sGC forms a key synapse integrating metabolic, energetic, and cell signaling, wherein ATP is the transmitter, allosteric inhibition the coupling mechanism, and regulated accumulation of cGMP the response.

Metabolically active cells with high-energy requirements are particularly susceptible to structural and functional impairment when deprived of oxygen and substrates obligatory for generating ATP (1, 2). Maintenance of homeostasis requires these cells to respond to rapidly fluctuating energy demands in the context of varying supplies of metabolic substrates. Tight coordination between energy supply and demand is predicated on efficient communication and integration between metabolism, the steady-state and local availability of high-energy phosphates, and signaling mechanisms regulating cell functions. Although specific components and their interactions that transduce metabolic and energetic signaling have been described (1), molecular mechanisms mediating their coordination with cellular signaling remain incompletely understood.

Production and release of NO represents one paracrine/autocrine mechanism coordinating energy supply and demand in tissues. Metabolic stress, such as ischemia, stimulates NO synthases to produce NO from arginine (3). In turn, NO regulates the supply of energy by improving the delivery of substrates and oxygen to deprived tissues (4–6), regulating the intracellular delivery of metabolic substrates (7–10), selection of substrates that support metabolism (6, 10–14), oxidation of metabolic substrates (15), generation of ATP by improving metabolic efficiency (16), and biogenesis of mitochondria (17). Conversely, NO reduces the demand for ATP by decreasing energy-consuming cell functions, for example, by reducing the activity of the contractile apparatus in muscle cells (ref. 18 and references therein). Moreover, in some models of severe hypoxic stress, NO induces complete and reversible metabolic stasis required to survive the insult (19). The importance of NO in defending against ischemia is underscored by its regulation of the transcription factor hypoxia inducible factor 1, a master regulator of cellular homeostasis in the context of oxygen insufficiency (20).

Coordination of energy supply and demand is mediated, in part, by NO activation of soluble guanylyl cyclase (sGC) and the associated accumulation of intracellular cGMP concentration ($[cGMP]_i$) (9, 10, 12, 15, 16, 18), yet the mechanisms coordinating cGMP-dependent and metabolic signaling, beyond the production of NO, remain undefined. Recently, a novel mechanism was identified by which adenine nucleotides inhibit GCs (21, 22) that is analogous to P site inhibition of adenylyl cyclases (23). Indeed, the two-substituted adenine nucleotides 2-methylthio-ATP and 2-chloro-ATP inhibit NO-dependent cGMP production by directly binding to sGC (22). Synthetic two-substituted adenine nucleotides presumably exploit allosteric mechanisms regulated by endogenous cell products. The present study revealed that ATP is the native ligand mediating adenine nucleotide-dependent inhibition of sGC by binding directly to an allosteric purinergic site on the enzyme. Moreover, intracellular levels of ATP are reciprocally coupled to responses of sGC to NO and accumulation of cGMP. Thus, sGC is an intracellular ATP sensor that couples NO-dependent cell functions with metabolic and energetic signaling.

Materials and Methods

Cell Culture. Human vascular smooth muscle cells (American Type Culture Collection) were maintained at 37°C in Ham's F12K (Mediatech, Herndon, VA) supplemented with 1.5 g/liter sodium bicarbonate, 10 mM Hepes, 10 mM 2-{[2-hydroxyl-1,1-bis(hydroxymethyl)ethyl]amino}ethane-sulfonic acid, 0.05 mg/ml ascorbic acid, 0.01 mg/ml insulin, 0.01 mg/ml transferrin, 10 ng/ml sodium selenite, 10% FBS (Mediatech), and 1% penicillin/streptomycin [10,000 units/ml penicillin, 10,000 μg/ml streptomycin (GIBCO)] in a humidified atmosphere of 5% CO_2. RFL-6 cells (American Type Culture Collection) were maintained at 37°C in Ham's F12K containing 20% FBS in a humidified atmosphere of 5% CO_2.

GC Activity. Crude (4–8 μg) or purified (10–20 ng) enzyme preparations were incubated for 5 min at 37°C in reactions (100 μl) containing 50 mM Tris·HCl (pH 7.5), $MgCl_2$ (3 mM in excess of nucleotide), GTP, sodium nitroprusside (SNP), ATP, and 8-azido-ATP, as indicated (21, 22). For crude sGC, reactions contained 500 μM isobutylmethylxanthine, 15 mM creatine phosphate, and 2.7 units of creatine phosphokinase, whereas for purified sGC they contained 0.5 mg/ml BSA and 1 mM DTT.

This paper was submitted directly (Track II) to the PNAS office.

Abbreviations: $[ATP]_i$, intracellular ATP concentration; $[Ca^{2+}]_i$, intracellular Ca^{2+} concentration; $[cGMP]_i$, intracellular cGMP concentration; MLC, myosin light chain; GC, guanylyl cyclase; sGC, soluble GC; SNP, sodium nitroprusside.

‡To whom correspondence should be addressed. E-mail: scott.waldman@jefferson.edu.

Enzyme reactions were terminated by the addition of 400 μl of 50 mM sodium acetate (pH 4.0) followed by boiling for 3 min, and cGMP was quantified by RIA. Enzyme reactions were performed in duplicate, and RIAs were analyzed in triplicate. Results reflect enzyme activities that were linear with respect to time and protein concentrations.

Photoaffinity Labeling of sGC with 8-Azido [γ-^{32}P]ATP. Purified sGC (1–2 μg) was incubated on ice with 50 μM 8-azido [γ-^{32}P]ATP (500–600 GBq/mmol; ICN) in 3 mM $MgCl_2$, 2.8 mM EDTA, 0.1 mM EGTA, and 25 mM triethanolamine, pH 7.4 in a final volume of 10 μl for 2 min in the dark. In some experiments, ATP or GTP was added 10 min before 8-azido [γ-^{32}P]ATP. After UV irradiation at 254 nm for 3 min, reactions were terminated with 50 mM DTT. Samples were resolved by electrophoresis on a 7.5% SDS-polyacrylamide gel and analyzed by staining with Gelcode blue (Pierce) followed by autoradiography.

ATP Quantification by Luciferase Assay. ATP was measured with an ATP Determination Kit (Molecular Probes), following the instructions of the manufacturer. Cells were lysed with 1× Passive Lysis Buffer (Promega), and lysates were diluted 1:10 by using the ATP Determination Kit reaction mix for a total volume of 200 μl. Luminescence was determined directly after the addition of the lysate to the reaction and was quantified in a 20/20 Luminometer (Turner Designs, Sunnyvale, CA). ATP concentrations in experimental samples were calculated by using an ATP standard curve.

Quantification of Intracellular cGMP. RFL-6 cells in 24-well plates at a density of 1–5 × 10^5 cells per well were preincubated for 30 min in Opti-MEM (GIBCO) containing 1 mM isobutylmethylxanthine and 5 mM ATP and/or 20 μM digitonin, where indicated. After preincubation, 400 μM Mg^{2+}, 100 μM GTP, and 125 μM SNP were added and incubations were continued for 15 min. Cells were lysed and cGMP was quantified by RIA (21, 22).

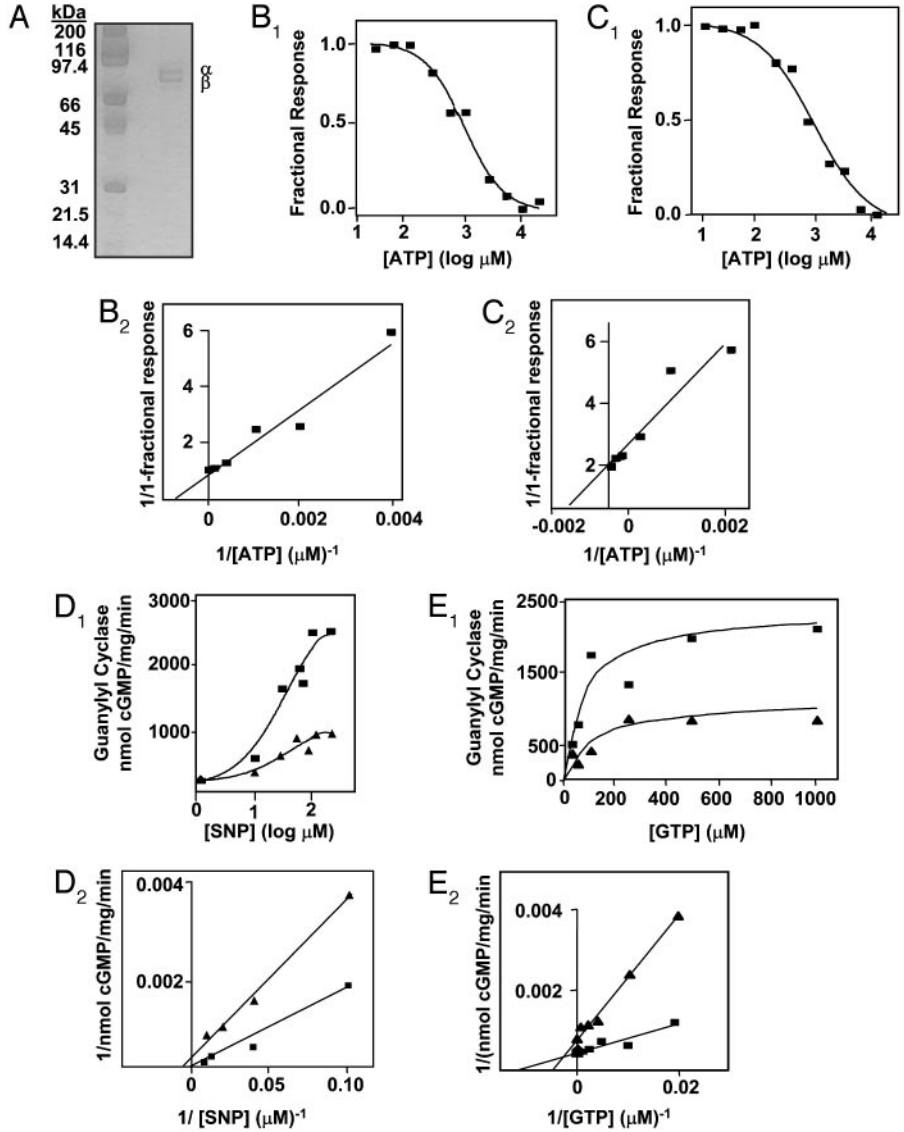

Fig. 1. ATP induces allosteric inhibition of sGC. (*A*) Preparations of purified human sGC are composed of α_1 and β_1 subunits. Purified sGC (1 μg) was analyzed by SDS/PAGE and stained with GelCode blue. (*B* and *C*) ATP inhibits SNP-stimulated crude (*B*) and purified (*C*) human sGC. Enzyme activity stimulated by 100 μM SNP was quantified in the presence of varying [ATP], as outlined in *Materials and Methods*. Reaction rates are expressed as fractional response (enzyme activity in the presence of nucleotide/enzyme activity in the absence of nucleotide). SNP-stimulated activities of crude and purified sGC were 158.3 ± 37.6 pmol cGMP min^{-1}·mg of $protein^{-1}$ and 3,205 ± 1,296 nmol cGMP min^{-1}·mg of $protein^{-1}$, respectively. (*D*) ATP decreases the efficacy, but not the potency, of SNP to activate purified human sGC. ■, SNP; ▲, SNP plus 1 mM ATP. (*E*) ATP inhibits purified human sGC by a mixed noncompetitive mechanism. ■, 100 μM SNP; ▲, 100 μM SNP plus 1 mM ATP. Reaction rates presented in curvilinear plots (B_1–E_1) were subjected to double reciprocal analysis (B_2–E_2).

Table 1. Potency (K_i) of adenine nucleotides to inhibit crude and purified human sGC

sGC	Nucleotide	K_i, μM
Vascular smooth muscle	ATP	1,035 ± 121
	$8N_3ATP$	ND
Purified human	ATP	2,249 ± 475
	$8N_3ATP$	2,326 ± 1,064

K_i values were extracted from nonlinear regression analyses of the sigmoidal plots of the concentration-dependence analyses of ATP inhibition of sGC activated by 100 μM SNP (see Fig. 1) or $8N_3ATP$ (see Fig. 2). Values are means ± SEM of three experiments performed in triplicate. ND, not determined.

Table 2. Kinetic parameters of purified sGC inhibited by ATP

	K_M, μM	V_{max}, nmoles cGMP produced/min per mg of protein
Control	156 + 5	750 + 111
1 mM ATP	356 + 86*	468 + 48*

K_M and V_{max} values were extracted from nonlinear regression analyses of Michaelis–Menten analyses of sGC stimulated by 100 μM SNP in the presence of different concentrations of Mg-GTP and in the absence or presence of 1 mM ATP (see Fig. 1). Values are means ± SEM of three experiments performed in triplicate. *$P < 0.05$ with respect to control (no added ATP) using a paired Student t test (two-tailed).

Inhibition of Mitochondrial ATP Synthesis by Oligomycin. RFL-6 cells plated in 24-well plates at a density of 1–5 × 10^5 cells per well were preincubated with Opti-MEM containing 1 mM isobutylmethylxanthine and 2.5% DMSO or 25 μM oligomycin, as indicated. After preincubation, cells were washed to remove oligomycin and incubated for various times in fresh media before 125 μM SNP was added and incubations were continued at 37°C, as indicated. Cells were lysed and cGMP was quantified by RIA (21, 22).

Miscellaneous. sGC ($\alpha_1\beta1$) purified to homogeneity by immunoaffinity chromatography from bovine lung was obtained from Alexis Biochemical (San Diego) (22). Human sGC ($\alpha_1\beta1$) was modified on the carboxyl terminus of the α_1 subunit with a hexahistidine tag, expressed in insect cells, and purified to homogeneity (Fig. 1*A*) by Ni affinity chromatography (24). sGC was prepared from vascular smooth muscle cells and rat lung as described (22). Isobutylmethylxanthine, GTP, SNP, PMSF, oligomycin, creatine phosphate, and creatine phosphokinase were obtained from Sigma. Digitonin, EDTA, ATP, DTT, and BSA were obtained from Fisher Scientific. Protein was quantified by the Bradford method (Bio-Rad or Pierce). All other reagents were from Fisher Scientific. All results are representative of at least three experiments performed in triplicate, unless otherwise indicated. Statistical significance was analyzed with Student's t test.

Results and Discussion

ATP inhibited basal (data not shown) and SNP-activated sGC extracted from human vascular smooth muscle cells (Fig. 1*B* and Table 1) or rat lung (data not shown) with a K_i of ≈1 mM and maximum inhibition (I_{max}) of 100%. Similarly, ATP inhibited basal (data not shown) and SNP-activated recombinant human $\alpha_1\beta1$ sGC (Fig. 1 *A* and *C* and Table 1) or bovine lung sGC (data not shown) purified to apparent homogeneity with a K_i of ≈2 mM and I_{max} of 100%. The identical potency and efficacy of ATP to inhibit crude and purified enzyme demonstrates that regulation reflects direct binding of nucleotide to sGC. Further, the sensitivity of sGC to ATP inhibition (K_i) in the context of homeostatic intracellular ATP concentration ($[ATP]_i$), ≈3 mM (25), suggests that cGMP responses to NO are repressed 60–75% under steady-state conditions. In contrast, ATP hydrolysis products, including ADP, AMP, and inorganic phosphate, did not alter NO activation of crude or purified sGC and did not competitively antagonize the inhibitory effect of ATP (data not shown). Thus, sGC appears to be a specific ATP sensor whose sensitivity falls within the dynamic range of (patho)physiological intracellular nucleotide concentrations.

SNP stimulated sGC with a potency that was identical in the absence (K_a = 34.0 ± 1.4 μM) or presence (K_a = 34.0 ± 5.7 μM) of ATP (Fig. 1*D*), suggesting that nucleotide inhibition did not reflect limitations in the concentration of NO available or its interaction with the heme prosthetic group of sGC. Rather, maximum activation of sGC by SNP decreased in the presence (E_{max} = 944 ± 67 nmol cGMP/mg of protein per min), compared to the absence (E_{max} = 2,407 ± 227 nmol cGMP/mg of protein per min; Fig. 1*D*), of ATP consistent with a model in which nucleotide allosterically regulates NO-activated sGC. Indeed, ATP inhibited NO-activated sGC by a mixed noncompetitive allosteric mechanism (Fig. 1*E* and Table 2) identical to that by which two-substituted nucleotides inhibit ligand-activated GC C and sGC (22), and P site inhibitors regulate ligand-activated adenylyl cyclases (23). Thus, ATP is the endogenous intracellular ligand mediating adenine nucleotide-dependent allosteric inhibition of GCs.

The kinetics of sGC inhibition by ATP are consistent with a model in which allosteric modulation is mediated by regulatory, rather than catalytic, nucleotide binding sites. Indeed, nucleotide cyclases exhibit rigid substrate selectivities at their catalytic sites, required to maintain signaling specificity and fidelity in an intracellular milieu in which these enzymes and substrate nucleotides are commingled (26). $8N_3ATP$, a photoaffinity analog of ATP and probe of protein nucleotide binding sites, was equipotent and equiefficacious compared to ATP in inhibiting SNP-stimulated sGC (Fig. 2 *A* and *B* and Table 1). Upon photoactivation, $8N_3[\gamma\text{-}^{32}P]ATP$ covalently labeled α and β subunits of sGC (Fig. 2*C*), suggesting that both subunits of sGC contribute residues to the allosteric nucleotide regulatory site, as they do to the substrate nucleotide catalytic site (26). ATP and

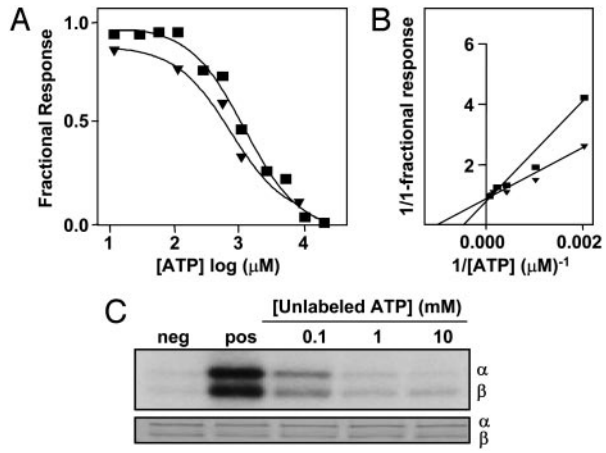

Fig. 2. Allosteric inhibition by adenine nucleotides is mediated by direct interaction with sGC. (*A* and *B*) ATP and $8N_3ATP$ inhibit purified human sGC stimulated by 100 μM SNP with comparable potencies. Reaction rates are expressed as fractional response, described in Fig. 1. ■, ATP; ▲, $8N_3ATP$. Reaction rates presented in sigmoidal plots (*A*) were subjected to double reciprocal analysis (*B*). (*C*) $8N_3ATP$ specifically interacts with a site on purified human sGC comprised of residues contributed by α_1- and β_1-subunits. Purified enzyme (1 μg) was incubated in the absence (pos, positive control) or presence of 0.1, 1, or 10 mM ATP for 10 min, followed by addition of 50 μM 8-azido $[\gamma^{32}P]ATP$. Reactions were incubated for 10 min and, unless otherwise indicated (neg, negative control), irradiated at 254 nm by 4.4 milliwatts/cm^2 for 2 min. Photoaffinity labeling was detected by autoradiography (*Upper*) and protein with GelCode blue (*Lower*).

GTP effectively antagonized binding of $8N_3[\gamma\text{-}^{32}P]ATP$ to α and β subunits (Figs. 2*C* and 3*A*), although GTP was a less potent antagonist than ATP (Fig. 3*A*). Moreover, GTP directly inhibited sGC (Fig. 3 *D* and *E*) by binding to (Fig. 3*A*) and competing with ATP at the same allosteric regulatory site (Fig. 3 *B–E*). Thus, allosteric inhibition of sGC is mediated by a regulatory purine nucleotide binding site formed by residues in the α and β subunits that preferentially binds ATP compared to GTP, in contrast to the rigid nucleotide specificity of the substrate catalytic site.

The role of sGC as an intracellular sensor of ATP, coupling metabolic and energetic fluxes to NO-dependent signaling was examined by using RFL-6 cells, a particularly responsive model of NO-induced $[GMP]_i$ accumulation (27). Regulation of sGC by $[ATP]_i$, rather than extracellular ATP, was highlighted by the inability of ATP to alter $[cGMP]_i$ accumulation in response to SNP when added to intact RFL-6 cells, reflecting the impermeability of the plasma membrane to polyanionic nucleotides (Fig. 4*A*). In contrast, extracellular ATP inhibited the accumulation of $[cGMP]_i$ induced by SNP in RFL-6 cells permeabilized with the detergent digitonin (Fig. 4*A*), which permits influx and intracellular accumulation of extracellular phosphorylated nucleotides (28). Coordination of sGC signaling and mitochondrial energy metabolism was probed by using oligomycin, a specific reversible inhibitor of the cGMP-regulated F_o cation channel, which is an essential component of the F_oF_1ATP synthase complex in inner mitochondrial membranes coupling aerobic substrate metabolism, oxidative phosphorylation, and ATP generation (29, 30). Indeed, oligomycin decreased steady-state concentrations of ATP ≈50% in intact RFL-6 cells (Fig. 4*B*), which enhanced SNP-induced accumulation of $[cGMP]_i$ ≈150% (Fig. 4*C*), without directly altering stimulation of sGC activity by NO (Fig. 4*D*). Moreover, reversal of ATP synthase inhibition by removing oligomycin resulted in the recovery of $[ATP]_i$, which was temporally coordinated with a return to baseline of SNP-induced accumulation of $[cGMP]_i$ (Fig. 4*E*). Regulation of SNP-induced cGMP production by steady-state concentrations of ATP in intact cells underscores the role of adenine nucleotide-dependent allosteric inhibition of sGC in mechanisms coupling NO signaling and cellular metabolism.

NO and cGMP are emerging as key mediators coordinating the supply and demand of ATP, particularly in tissues with high-energy requirements, in which structural and functional integrity can be compromised by metabolic fluctuations. The role of NO and sGC signaling in modulating ATP demand is exemplified in smooth and cardiac muscle. Contractility reflects the integration of synergistic and antagonistic signals regulating intracellular Ca^{2+} concentration ($[Ca^{2+}]_i$) (ref. 18 and references therein). Contractile signals elevate $[Ca^{2+}]_i$ and/or sensitize myofibrils to Ca^{2+}. Conversely, relaxation signals decrease $[Ca^{2+}]_i$ and/or desensitize the contractile apparatus to Ca^{2+}. The net effect of these opposing processes is phosphorylation of myosin light chains (MLCs) by MLC kinase, which contributes to contraction, or dephosphorylation of MLC by MLC phosphatase, which contributes to relaxation, respectively. NO, produced in response to metabolic stress (3), activates sGC and the accumulation of $[cGMP]_i$, inhibiting energy-consuming contraction and promoting energy-conserving relaxation (18). Relaxation induced by cGMP, and the associated conservation of energy stores, is effected by desensitization of the contractile apparatus to $[Ca^{2+}]_i$, by activation of MLC phosphatase, which decreases MLC phosphorylation, and by uncoupling force generation from MLC phosphorylation. Moreover, cGMP lowers $[Ca^{2+}]_i$ by reducing Ca^{2+} influx through L-type Ca^{2+} channels, increasing Ca^{2+} efflux through a Ca^{2+}-pumping ATPase and a Na^+/Ca^{2+} exchanger, and increasing intracellular Ca^{2+} seques-

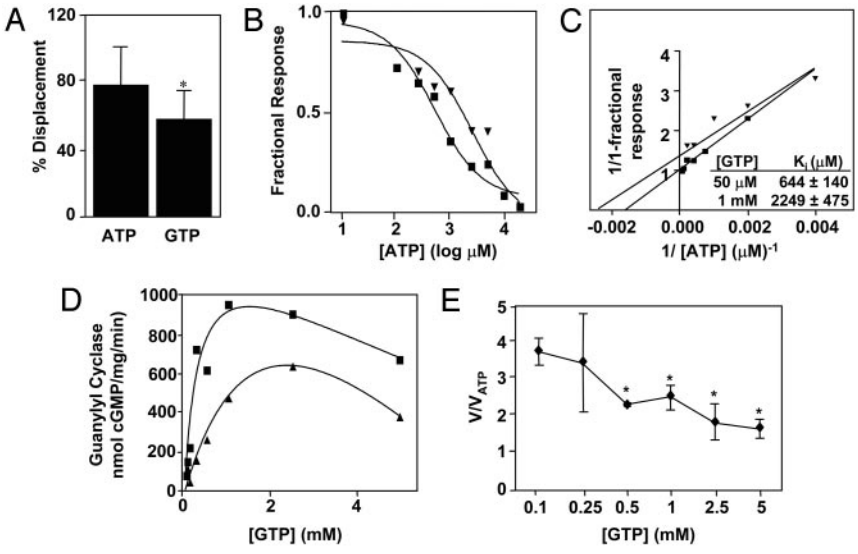

Fig. 3. Inhibition of sGC by ATP is mediated by an allosteric purine nucleotide binding site. (*A*) Binding of $8N_3ATP$ to human purified sGC is antagonized by purine nucleotides with a rank order potency of ATP > GTP. Enzyme (1 μg) was preincubated with 1 mM ATP or GTP and photoaffinity-labeled with 50 μM 8-azido $[\gamma^{32}P]ATP$, as outlined in Fig. 2. Relative incorporation of radioactivity into sGC in the presence of unlabeled nucleotides is expressed as the percentage of displacement compared to incubations that omitted those nucleotides. (*B–E*) GTP antagonizes inhibition of sGC by ATP by productively interacting with the allosteric nucleotide binding site. (*B*) GTP shifted the concentration dependence of ATP inhibition to the right, reflecting the ability of GTP to compete with ATP for binding to the nucleotide regulatory site. Enzyme activity stimulated by 100 μM SNP was quantified by using 50 μM (■) or 1 mM (▲) GTP. Reaction rates are expressed as fractional response, described in Fig. 1. Reaction rates of purified sGC stimulated by SNP with 50 μM GTP or 1 mM GTP were 619 ± 76 and 3,205.2 ± 1,296 nmol cGMP $min^{-1}\cdot mg^{-1}$ of protein, respectively. Reaction rates presented in sigmoidal plots (*B*) were subjected to double reciprocal analysis (*C*). The K_i of ATP, estimated by nonlinear regression analyses of sigmoidal plots ($n = 3$), was significantly ($P < 0.05$) greater when higher concentrations of GTP were used (*Inset*). (*D*) Purified human sGC activity stimulated by 100 μM SNP was quantified by using a range of [GTP] in the presence (▲) or absence (■) of 1 mM ATP. Indeed, [GTP] >1 mM directly inhibit, and attenuate the ability of ATP to inhibit, sGC. The concentration dependence of GTP to attenuate inhibition of sGC by ATP, reflecting productive interaction of GTP with the allosteric nucleotide regulatory site, is illustrated by plotting relative enzyme activities (activity in the absence of ATP/activity in the presence of ATP; V/V_{ATP}) (*E*). In *A* and *E*, results represent the means ± SEM of three experiments. *, $P < 0.05$ compared to 0.1 mM GTP.

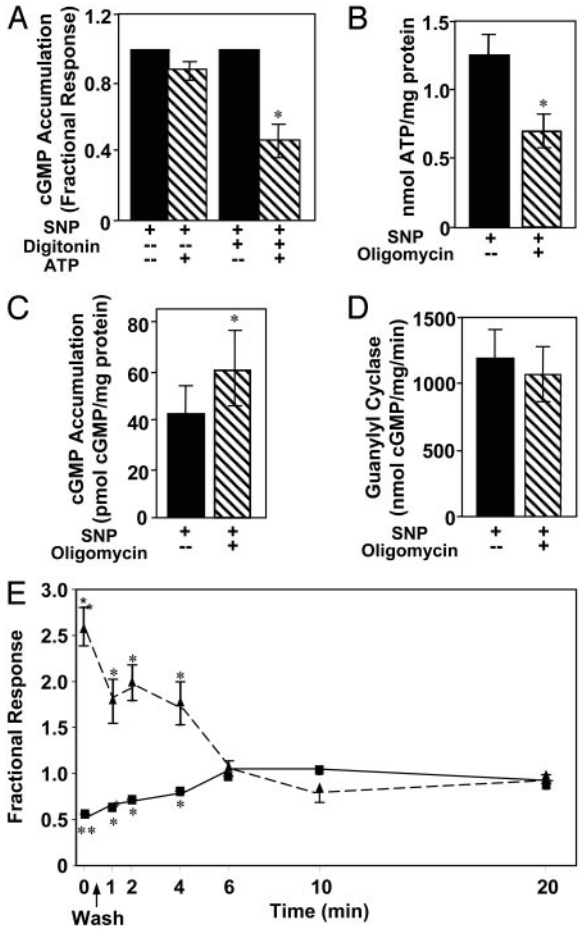

Fig. 4. Mitochondrial ATP regulates SNP-induced intracellular accumulation of cGMP. (*A*) ATP inhibits SNP-induced cGMP accumulation in RFL-6 cells only when $[\text{nucleotide}]_i$ are clamped by permeabilizing cells with digitonin. cGMP accumulation in RFL-6 cells induced by 125 μM SNP was quantified in the presence or absence of 5 mM ATP and 20 μM digitonin. (*B–E*) Oligomycin, an inhibitor of mitochondrial oxidative phosphorylation, reduces $[\text{ATP}]_i$ (*B*), which is associated with an increase in SNP-induced accumulation of cGMP (*C*) in RFL-6 cells. In contrast, oligomycin did not affect the ability of SNP to activate purified human sGC (*D*). Removal of oligomycin (wash) produced a coordinated time-dependent recovery of $[\text{ATP}]_i$ (■) and SNP-induced accumulation of cGMP (▲) (*E*). $[\text{ATP}]_i$ and $[\text{cGMP}]_i$ were quantified after incubation for 1 (*E*) or 15 (*B–D*) min with 125 μM SNP, with or without preincubation for 60 (*E*) or 90 (*B–D*) min with 25 μM oligomycin. Results represent the means ± SEM of three independent experiments. *, $P < 0.05$; **, $P < 0.01$.

tration by activating the Ca^{2+}-pumping ATPase in the sarcoplasmic reticulum and inhibiting inositol 1,4,5-trisphosphate-dependent Ca^{2+} mobilization. The integrated reduction in myofibril contractility, induced by cGMP in response to metabolic stress, decreases tissue indices of energy demand, including force of contraction (31), tension (32), fractional shortening (33), and maximum rate of shortening (34).

Beyond vascular smooth muscle relaxation associated with improved tissue perfusion (4–6), NO also regulates the supply of cellular energy in the face of a metabolic challenge. Thus, NO and the associated production of cGMP decrease the transport, availability through glycogenolysis, and metabolic activation of glucose (9, 10). Conversely, cGMP increases the transport and utilization of fatty acids as metabolic substrates, which are associated with a more favorable respiratory quotient (6, 14). Further, cGMP shifts the balance of flux of metabolic substrates from glycolysis to oxidative phosphorylation, optimizing ATP generation (15). The role of cGMP in regulating the supply of cellular energy is underscored by the recent discovery that NO induces mitochondrial biogenesis in a variety of cells by activation of sGC associated with cGMP-dependent induction of peroxisome proliferator-activated receptor γ coactivator 1α, a master regulator of mitochondrial biogenesis (17). Indeed, NO and cGMP regulate mitochondrial biogenesis in response to hypothermic stress and interruption of that signaling mechanism disrupts body energy balance (17). Moreover, NO activation of sGC and the associated accumulation of $[\text{cGMP}]_i$ contribute to metabolic remodeling important in ischemic preconditioning in the cardiovascular and central nervous systems (4, 5). Together, the coordinated reduction in cell functions demanding energy and increase in mechanisms supplying energy mediated by NO and cGMP improve steady-state ATP levels (35) and survival (36–38) in the context of a metabolic challenge.

Defending structural and functional integrity in the face of metabolic challenges in cells with high-energy requirements is predicated on tight coordination of metabolic, energetic, and cell signaling. Well described mechanisms control the selection of substrates and routing of their flux through anaerobic and aerobic metabolic pathways, ultimately leading to oxidative phosphorylation and the production of ATP in mitochondria (1, 6, 10–14, 39). More recently, the importance of spatially organized intracellular enzymatic networks supporting high-energy phosphoryl transfer in coupling ATP generation in mitochondria on the one hand, and ATP-consuming or -sensing processes on the other, has emerged (1). This concept emphasizes the requirement of energetic signaling to maintain the balance between cellular ATP production and consumption. Although the individual components and their interactions regulating metabolic, energetic, and cellular signaling have been described, the precise mechanisms orchestrating their integration remain to be defined. Specifically, whereas the NO-sGC-cGMP pathway serves as one downstream effector system coupling alterations in energy levels to compensatory responses, the mechanistic interface between energetic and cGMP signaling, beyond NO production, has been unclear. Here, we demonstrate that sGC is an intracellular purine nucleotide sensor, with a preference for ATP > GTP, whose responsiveness to NO is set by physiological $[\text{ATP}]_i$. Indeed, alterations in $[\text{ATP}]_i$, either by permeabilization followed by nucleotide clamping, or by metabolic inhibition of mitochondrial ATP production, regulated the responsiveness of sGC to NO activation and cGMP production. These observations support a model in which $[\text{ATP}]_i$ serves as a "gain control" for the NO sensitivity of sGC. At normal homeostatic concentrations of $[\text{ATP}]_i$, sGC is repressed (≥60%, see Fig. 1) and resistant to NO activation. In the face of a metabolic challenge, in which $[\text{ATP}]_i$ can decrease 20-fold (40, 41), sGC is derepressed, amplifying cGMP responses to NO. Thus, sGC forms one key synapse coordinating the flow of information through metabolic, energetic, and cell signaling pathways, wherein nucleotide-dependent allosteric inhibition is the mechanism mediating that coordination, and ATP is the messenger bridging that synapse.

In summary, these studies revealed that sGC is a physiological sensor of $[\text{ATP}]_i$, which couples NO signaling and cellular energy homeostasis through nucleotide-dependent allosteric regulation. Amplification of NO signaling by sGC, reflecting allosteric derepression by reductions in $[\text{ATP}]_i$, likely underlies the previously unexplained augmentation of NO-dependent cGMP production in anoxic cardiomyocytes (42–44) and vascular relaxation induced by hypoxia (45). Repression of sGC by $[\text{ATP}]_i$ reflects a global mechanism coordinating cellular cGMP responses and metabolic and energetic signaling because adenine nucleotides allosterically regulate GC isoforms localized in the major subcellular compartments (21, 22, 28). Although the present study demonstrates that $[\text{ATP}]_i$ is the proximal messenger bridging the synapse between cellular metabolism and cGMP production, future studies will define the precise enzymatic

networks mediating high-energy phosphoryl transfer that couple ATP generation in mitochondria to ligand-dependent GC signaling in the cytosol and at the membrane (1).

This work was supported by grants from the National Institutes of Health (HL65921, CA7512, and CA7966) and Targeted Diagnostics and Therapeutics (to S.A.W.), the Landenberger Foundation (to G.M.P.), and the J. S. Dunn and Welch Foundations, the National Institutes of Health (GM61731 and HL64221), the National Aeronautics and Space Administration, and the Department of Defense (to E.M. and F.M.). I.R.-S. was supported by National Institutes of Health Minority Supplement HL59214-0151. S.R.T. was enrolled in a National Institutes of Health-supported Institutional K30 Training Program in Human Investigation (K30 HL004522) and was supported by National Institutes of Health Institutional Training Grant T32 GM08562. S.A.W. is the Samuel M. V. Hamilton Professor of Medicine at Thomas Jefferson University.

1. Dzeja, P. P. & Terzic, A. (2003) *J. Exp. Biol.* **206,** 2039–2047.
2. Lee, J. M., Grabb, M. C., Zipfel, G. J. & Choi, D. W. (2000) *J. Clin. Invest.* **106,** 723–731.
3. Zweier, J. L., Wang, P. & Kuppusamy, P. (1995) *J. Biol. Chem.* **270,** 304–307.
4. Park, K. M., Byun, J. Y., Kramers, C., Kim, J. I., Huang, P. L. & Bonventre, J. V. (2003) *J. Biol. Chem.* **278,** 27256–27266.
5. Kawabata, H. & Ishikawa, K. (2003) *Hypertens. Res.* **26,** 107–110.
6. Bernstein, R. D., Ochoa, F. Y., Xu, X., Forfia, P., Shen, W., Thompson, C. I. & Hintze, T. H. (1996) *Circ. Res.* **79,** 840–848.
7. Roberts, C. K., Barnard, R. J., Scheck, S. H. & Balon, T. W. (1997) *Am. J. Physiol.* **273,** E220–E225.
8. Young, M. E., Radda, G. K. & Leighton, B. (1997) *Biochem. J.* **322,** 223–228.
9. Depre, C., Gaussin, V., Ponchaut, S., Fischer, Y., Vanoverschelde, J. L. & Hue, L. (1998) *Am. J. Physiol.* **274,** H1443–H1449.
10. Tada, H., Thompson, C. I., Recchia, F. A., Loke, K. E., Ochoa, M., Smith, C. J., Shesely, E. G., Kaley, G. & Hintze, T. H. (2000) *Circ. Res.* **86,** 270–274.
11. Ljusegren, M. E. & Axelsson, K. L. (1993) *Pharmacol. Toxicol.* **72,** 56–60.
12. Beitner, R., Haberman, S. & Cycowitz, T. (1977) *Biochim. Biophys. Acta* **482,** 330–340.
13. Khedara, A., Kawai, Y., Kayashita, J. & Kato, N. (1996) *J. Nutr.* **126,** 2563–2567.
14. Recchia, F. A., McConnell, P. I., Loke, K. E., Xu, X., Ochoa, M. & Hintze, T. H. (1999) *Cardiovasc. Res.* **44,** 325–332.
15. Young, M. E. & Leighton, B. (1998) *FEBS Lett.* **424,** 79–83.
16. Shen, W., Tian, R., Saupe, K. W., Spindler, M. & Ingwall, J. S. (2001) *Am. J. Physiol.* **281,** H838–H846.
17. Nisoli, E., Clementi, E., Paolucci, C., Cozzi, V., Tonello, C., Sciorati, C., Bracale, R., Valerio, A., Francolini, M., Moncada, S. & Carruba, M. O. (2003) *Science* **299,** 896–899.
18. Lucas, K. A., Pitari, G. M., Kazerounian, S., Ruiz-Stewart, I., Park, J., Schulz, S., Chepenik, K. P. & Waldman, S. A. (2000) *Pharmacol. Rev.* **52,** 375–414.
19. Teodoro, R. O. & O'Farrell, P. H. (2003) *EMBO J.* **22,** 580–587.
20. Sandau, K. B., Fandrey, J. & Brune, B. (2001) *Blood* **97,** 1009–1015.
21. Parkinson, S. J., Carrithers, S. L. & Waldman, S. A. (1994) *J. Biol. Chem.* **269,** 22683–22690.
22. Ruiz-Stewart, I., Kazerounian, S., Pitari, G. M., Schulz, S. & Waldman, S. A. (2002) *Eur. J. Biochem.* **269,** 2186–2193.
23. Dessauer, C. W., Tesmer, J. J., Sprang, S. R. & Gilman, A. G. (1999) *Trends Pharmacol. Sci.* **20,** 205–210.
24. Lee, Y. C., Martin, E. & Murad, F. (2000) *Proc. Natl. Acad. Sci. USA* **97,** 10763–10768.
25. Traut, T. W. (1994) *Mol. Cell Biochem.* **140,** 1–22.
26. Sunahara, R. K., Beuve, A., Tesmer, J. J., Sprang, S. R., Garbers, D. L. & Gilman, A. G. (1998) *J. Biol. Chem.* **273,** 16332–16338.
27. Ishii, K., Sheng, H., Warner, T. D., Forstermann, U. & Murad, F. (1991) *Am. J. Physiol.* **261,** H598–H603.
28. Parkinson, S. J. & Waldman, S. A. (1996) *Biochemistry* **35,** 3213–3221.
29. Boyer, P. D. (1997) *Annu. Rev. Biochem.* **66,** 717–749.
30. McGeoch, J. E. & Guidotti, G. (2001) *Eur. J. Paediatr. Neurol.* **5,** Suppl. A, 147–150.
31. Wegener, J. W., Nawrath, H., Wolfsgruber, W., Kuhbandner, S., Werner, C., Hofmann, F. & Feil, R. (2002) *Circ. Res.* **90,** 18–20.
32. Machtens, S., Ckert, S., Stief, C. G., Tsikas, D., Frlich, J. C. & Jonas, U. (2003) *Urology* **61,** 479–483.
33. Ullrich, R., Scherrer-Crosbie, M., Bloch, K. D., Ichinose, F., Nakajima, H., Picard, M. H., Zapol, W. M. & Quezado, Z. M. (2000) *Circulation* **102,** 1440–1446.
34. Zhang, Q., Yan, L., Weiss, H. R. & Scholz, P. M. (2002) *Pharmacology* **64,** 106–112.
35. Pulido, E. J., Shames, B. D., Selzman, C. H., Barton, H. A., Banerjee, A., Bensard, D. D. & McIntyre, R. C., Jr. (1999) *Am. J. Physiol.* **277,** L769–L776.
36. Guth, B. D., Schulz, R. & Heusch, G. (1993) *Circulation* **87,** Suppl. IV, 35–42.
37. Schleiffer, R. & Raul, F. (1996) *Gut* **39,** 194–198.
38. Rivera-Chavez, F. A., Toledo-Pereyra, L. H., Dean, R. E., Crouch, L. & Ward, P. A. (2001) *J. Invest. Surg.* **14,** 267–273.
39. Cortassa, S., Aon, M. A., Marban, E., Winslow, R. L. & O'Rourke, B. (2003) *Biophys. J.* **84,** 2734–2755.
40. Shimizu, H., Graham, S. H., Chang, L. H., Mintorovitch, J., James, T. L., Faden, A. I. & Weinstein, P. R. (1993) *Brain Res.* **605,** 33–42.
41. Jones, R. N., Attarian, D. E., Currie, W. D., Olsen, C. O., Hill, R. C., Sink, J. D. & Wechsler, A. S. (1981) *J. Thorac. Cardiovasc. Surg.* **81,** 264–273.
42. Metsa-Ketela, T., Laustiola, K., Lilius, E. M. & Vapaatalo, H. (1981) *Acta Pharmacol. Toxicol.* **48,** 311–319.
43. Geisbuhler, T. P. & Schwager, T. L. (1996) *J. Mol. Cell. Cardiol.* **28,** 1857–1866.
44. Agullo, L., Garcia-Dorado, D., Escalona, N., Ruiz-Meana, M., Inserte, J. & Soler-Soler, J. (2003) *Am. J. Physiol.* **284,** H2170–H2176.
45. Inoue, M., Nishikawa, M., Sato, E. F., Ah-Mee, P., Kashiba, M., Takehara, Y. & Utsumi, K. (1999) *Free Radical Res.* **31,** 251–260.